

Catalysis of the Silica Sol–Gel Process by Divalent Transition Metal Bis(acetylacetonate) Complexes

Elizabeth I. Mayo, Duke D. Pooré, and A. E. Stiegman*

Department of Chemistry, Florida State University, Tallahassee, Florida 32306

Received March 11, 1999

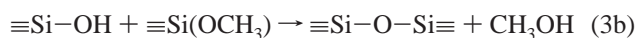
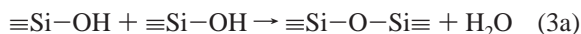
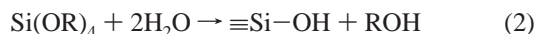
Transition metal bis(acetylacetonate) complexes of Co(II), Ni(II), Cu(II), and Zn(II) have been found to be active catalysts for the sol–gel process. The catalytic activity of these complexes decreases in going from Co(II) to Zn(II) and is highest for the acetylacetonate ligand system. ^{29}Si NMR studies show that the complexes act primarily as condensation catalysts and are, in that regard, similar to Brønsted bases such as hydroxide. Mechanistically, however, they appear to differ significantly from hydroxide in how they induce condensation. This is revealed in the catalyst concentration dependence, which is $1/2$ order for the metal complexes and 1st order in hydroxide. Differences are also apparent in the thermochemical parameters that indicate that the metal complexes act to increase the entropy of the transition state leading to condensation. The catalytic activity is proportional to the degree of ligand dissociation of the metal complex, and experiments suggest that the active catalytic species is specifically the first dissociation product, $\text{M}^{\text{II}}(\text{acac})^+$.

Introduction

The sol–gel process is of considerable interest as a synthetically flexible, low-temperature approach to the fabrication of metal and semi-metal oxide glasses and ceramics.^{1,2} The use of the sol–gel process to produce amorphous silica glasses (xerogels) commonly involves the reaction of silicon tetraalkoxides with water in an alcoholic medium: the net reaction of which is represented by reaction 1, where “R” is usually methyl or ethyl.³ The net reaction occurs through two steps, hydrolysis



(eq 2) and condensation (eq 3).³



Hydrolysis involves the attack of the water on the silicon alkoxide to yield a silanol, while condensation, which forms Si–O–Si linkages, occurs by either a water (eq 3a) or alcohol (eq 3b) producing pathway.³ While the sol–gel reaction proceeds as written in reaction 1, it is generally slow and, in practice, catalysts such as HCl and NH_4OH are usually employed.⁴ These catalysts accelerate the reaction quite differently in terms of the constitutive reactions of the sol–gel process. Acids tend to accelerate the hydrolysis (eq 2), while bases tend to catalyze the condensation (eq 3). This difference in reactivity dramatically affects the reaction kinetics and, ultimately, the final properties of the xerogel.^{5–8}

Because of their general utility, Brønsted acid and base catalysis of the silica sol–gel process has been well studied and the mechanistic aspects of their reactivity comprehensively explained.^{5–8} In general, however, other catalysts for the process and, in particular, transition metal based catalysts have not been extensively reported, although the observation that certain metal ions inhibit or accelerate the process has been made.⁹ Recently, as part of our studies of multicomponent metal–silica sol–gel systems, we observed that the series of first-row transition metal bis(acetylacetonate) (acac) complexes ($\text{M}(\text{II})(\text{acac})_2$; $\text{M}(\text{II}) = \text{Co}(\text{II}), \text{Ni}(\text{II}), \text{Cu}(\text{II}), \text{Zn}(\text{II})$) were catalysts for the sol–gel process with some of these complexes yielding gelation times for tetramethyl orthosilicate (TMOS) that were comparable to those of Brønsted acids or bases. That metal complexes of this type are facile catalysts is of interest, especially in light of the fact that they are often used to introduce late transition metals into the xerogel matrix. We present here a study of the catalytic activity of these complexes aimed at understanding their overall efficiency and ascertaining some of the mechanistic aspects of their activity.

Experimental Section

Tetramethyl orthosilicate (TMOS) and anhydrous Ni(II), Co(II), and Cu(II) 2,4-pentanedionate (acetylacetonate) were purchased from Gelest. $\text{Zn}^{\text{II}}(\text{acac})_2$ dihydrate, $\text{Cr}^{\text{III}}(\text{acac})_3$, NiNO_3 and Ni(II) acetate were purchased from Aldrich. Methanol, which was the solvent used in all experiments, NaOH, and HCl (concentrated, reagent grade) were purchased from Fisher and used as received.

^{29}Si NMR Spectroscopy. All reactions were carried out using deionized water (18.0 mho; Barnsted E-Pure system). NMR experiments

- (1) Ulrich, D. R. *J. Non-Cryst. Solids* **1988**, *100*, 174.
- (2) Mackenzie, J. D. *J. Non-Cryst. Solids* **1988**, *100*, 162.
- (3) Brinker, C. J.; Scherer, G. W. *Sol–Gel Science*; Academic Press: San Diego, CA, 1990; p 108.
- (4) Reference 3, p 130.

- (5) Brinker, C. J.; Keefer, K. D.; Schaefer, D. W.; Ashley, C. S. *J. Non-Cryst. Solids* **1982**, *48*, 47.
- (6) Brinker, C. J.; Keefer, K. D.; Schaefer, D. W.; Assink, R. A.; Kay, B. D.; Ashley, C. S. *J. Non-Cryst. Solids* **1984**, *63*, 45.
- (7) Brinker, C. J.; Scherer, G. W. *J. Non-Cryst. Solids* **1985**, *70*, 301.
- (8) Brinker, C. J.; Scherer, G. W. In *Ultrastructure Processing of Advanced Materials*; Hench, L. L., Ulrich, D. R., Eds.; John Wiley: New York, 1984; p 43.
- (9) Bansal, N. P. *NASA Technical Memorandum TM-101380*; NTIS: Springfield, VA.

were performed on a Bruker AC 300 NMR spectrometer. Solutions were made up and run in glass 10-mm NMR tubes. The broad band probe was tuned to 59.6 MHz for the ^{29}Si nucleus. A 4.5 μs pulse width (45° tip angle) was used with a 3 s repetition rate for 100 transients. All spectra were secondarily referenced to tetramethylsilane (TMS). The resonance from the silicon in the glass NMR tube was a broad band upfield (−110.3 ppm) from the resonance of TMOS (−77.8 ppm) and the majority of relevant intermediates. Due to the long relaxation times of the ^{29}Si nucleus, $\text{Cr}^{\text{III}}(\text{acac})_3$ (0.015 M) was used to act as a relaxation agent. Control experiments show that $\text{Cr}^{\text{III}}(\text{acac})_3$ is inert in the sol–gel process and no reactivity was seen between it and the M(II) bis(acac) compounds. All ^{29}Si resonances for the sol–gel process are specified using the conventional Q^n notation, where n indicates the number of bridging oxygens (−OSi) around the silicon. These resonances for a Si^* designated Q^1 , Q^2 , Q^3 , and Q^4 therefore correspond to $\text{Si}^*(-\text{OSi})_1$, $\text{Si}^*(-\text{OSi})_2$, $\text{Si}^*(-\text{OSi})_3$, and $\text{Si}^*(-\text{OSi})_4$, respectively.^{10,11} The resonances from a Q^4 silicon overlaps with the Q^4 resonances in the NMR tube and the glass housing surrounding the coil in the NMR probe.

Viscometry. Viscometry studies were performed on a Brookfield model DV-II+ rotating spindle viscometer using a small sample adapter (SC4–21SD spindle) to obtain absolute viscosity. Temperature was maintained (± 0.02 °C) with a water jacket through which 2-propanol, thermostated using a Haake A80 recirculating temperature control bath, was passed. A 3 rpm shear rate was used for all measurements, and the molarity of the silicon alkoxide was kept constant at 2.05 M. The molarity of the water varied according to the experiment run and is reported as a molar ratio to silicon alkoxide.

Gelation Times. The gelation point was determined by two different methods. In viscometry measurements, gelation is defined as the point where the viscosity just exceeds the range of the instrument.¹² Multiple determinations by this method of gelation times for identical samples of the catalysts studied here were found to be reproducible with a standard deviation of $\pm 5\%$. This standard deviation was used in all error analysis involving gelation times. Because of the reproducibility of gelation times determined by viscometry, it was the method used in all quantitative determinations.

For more qualitative comparisons, the gelation times were determined by visually monitoring fluid flow in static sol–gel solutions sealed in 4 mL styrene cuvettes. Under these conditions the gelation time is defined as the point at which, upon inversion of the container, the solution did not flow. Because of the differences in the definition of the gelation point, the two methods yield different gelation times for the same solution. For example, gelation of $\text{Ni}(\text{acac})_2$ -catalyzed sol–gel solutions at room temperature were determined to be 122 min by viscometry and 160 min by the visual method. The method by which the gelation times is determined is specified in the text, and all comparisons made between gelation times were between times determined by the same method.

Gas Physisorption Measurement. Nitrogen adsorption–desorption measurements were performed at 77 K on a Micromeritics ASAP 2010 sorptometer. Prior to measurement, all samples, previously dried at 500 °C, were degassed for 12 h at 150 °C. Adsorption and desorption isotherms over a range of relative pressure (P/P°) of 0.01–0.95 were collected for all samples.¹³ Surface areas were determined from the Brunauer–Emmett–Teller (BET) equation in a relative pressure range between 0.01 and 0.10.¹⁴ Pore volumes were determined from the whole isotherm from density functional theory using a slit-pore model.¹⁵ Micropore surface areas were estimated from t -plot analysis in the range $0.30 < t < 0.50$ nm using the Harkins–Jura correlation.^{16,17} All isotherms are described using IUPAC nomenclature.¹⁸

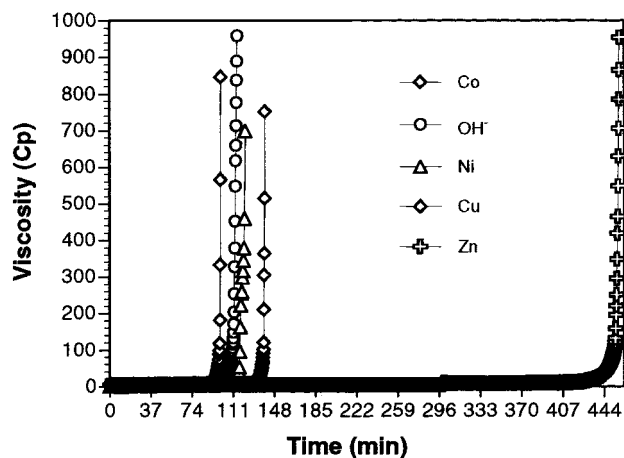


Figure 1. Temporal evolution of the viscosity of an aqueous 2.05 M tetramethyl orthosilicate solution (5:1 water/silicon) catalyzed with 2.0 mM Co(II), Ni(II), Cu(II), and Zn(II) bis(acetylacetonate) complexes and NaOH.

Table 1. Gelation Times of Tetramethyl Orthosilicate in the Presence of Various Catalysts

catalyst ^a	gelation time (min) ^b ($\pm 5\%$)
Co(acac) ₂	96
OH [−]	115
Ni(acac) ₂	122
Cu(acac) ₂	140
Zn(acac) ₂	458
none	1473

^a Catalyst concentration is 2 mM. ^b Obtained from viscometry (see Experimental Section).

pH Measurements. The pH of aqueous solutions of the metal complexes was determined using a calibrated Accumet 950 pH meter equipped with a Corning Semimicro Combination pH electrode. All measurements were carried out using deionized water (18.0 mho; Barnsted E-Pure system) which had been boiled to attain a pH of 7. The pH was measured of aqueous solution containing metal complexes dissolved to attain a concentration of 2 mM with care taken to exclude dissolution of atmospheric CO₂.

Metal Speciation Calculations. The concentrations of the metal species in aqueous solution were calculated from the equilibrium expressions and relevant mass and charge balance equations. The simultaneous equations were solved analytically on a computer using MAPLE math analysis software. For every calculation involving a starting concentration of added metal complex, seven solutions were obtained for all the concentrations, only one of which was real valued and positive.

Results and Discussion

Kinetics and Catalytic Activity of $M^{\text{II}}(\text{acac})_2$ Complexes.

The temporal evolution of the viscosity of a series of aqueous alcoholic TMOS (2.05 M; 5:1 water/silicon) solutions made with 2.0 mM Co(acac)₂, Ni(acac)₂, Cu(acac)₂, Zn(acac)₂, and OH[−] is shown in Figure 1. The gelation times, obtained from viscometry, are tabulated in Table 1. Clearly, all of the metal complexes act as catalysts for the process by inducing gelation significantly faster than an uncatalyzed control. Of the metal complexes investigated, the bis(acetylacetonate) complexes of cobalt and nickel were the most efficient, yielding gelation times that were comparable to hydroxide under identical conditions. The catalytic activity was observed to increase going from left to right across the periodic table with Co > Ni > Cu \gg Zn.

(10) Enghardt, V. G.; Altenburg, W.; Hoebbel, D.; Wieker, W. Z. *Z. Anorg. Allg. Chem.* **1977**, *418*, 43.

(11) Reference 3, p 164.

(12) Debsikdar, J. C. *Adv. Ceram. Mater.* **1986**, *1*, 93

(13) Gregg, S.; Sing, K. S. W. *Adsorption, Surface Area, and Porosity*; Academic Press: San Diego, CA, 1997.

(14) Brunauer, S.; Emmett, P. H.; Teller, E. *J. Am. Chem. Soc.* **1938**, *60*, 309.

(15) Olivier, J. P. *J. Por. Mater.* **1995**, *2*, 9.

(16) Lippens, B. C.; Linsen, B. G.; de Boer, J. H. *J. Catal.* **1964**, *3*, 32.

(17) Harkins, W. D.; Jura, G. *J. Chem. Phys.* **1943**, *11*, 431.

(18) Sing, K. S. W.; Everett, D. H.; Haul, R. A. W.; Moscou, L.; Pierotti, R.; Rouqu  rol, J.; Siemieniewska, T. A. *Pure Appl. Chem.* **1985**, *57*, 603.

Table 2. Gelation Times for Tetramethyl Orthosilicate Catalyzed by Ni(II) Complexes

metal complex ^a	gelation time (min) ^b
Ni(acac) ₂	150
Ni(acetate) ₂	192
Ni(H ₂ O) ₆ ²⁺	1020
no catalyst	1650

^a [Catalyst] = 0.002 M. ^b Gelation times determined from flow properties of static solutions (see Experimental Section).

The catalytic activity exhibited by these complexes appears to be quite dependent on the ligand system. Simple hexaquo complexes such as Ni(H₂O)₆²⁺, introduced as the nitrate salt, showed very little catalytic activity (Table 2). Other organic ligand systems such as carboxylates showed significant catalytic activity though, for a given metal, none exceeded acetylacetonate (Table 2).

Activity of M^{II}(acac)₂ Complexes as Condensation Catalysts. Brønsted acids and bases catalyze the sol–gel process due to their ability to drive hydrolysis (eq 2) and condensation (eq 3) reactions of the silicon alkoxide, respectively. In the former case, protonation of the silicon alkoxide by the acid makes the alkoxide a better leaving group, and hence, it is easily displaced by water.⁴ Conversely, hydroxide favors the formation of siloxides, SiO⁻, which readily displace alkoxy or hydroxy groups on silicon to form Si–O–Si bonds.⁴ These two types of catalytic activity can be distinguished by the product distribution of the silica species as the reaction evolves. With acid, the starting tetramethyl orthosilicate is rapidly hydrolyzed before it begins to condense. Since condensation is rate limiting, progressively more condensed species gradually emerge over time. This can be observed directly by ²⁹Si NMR spectroscopy, where all degrees of hydrolysis (Si(OR)_{4-x}(OH)_x, x = 1–4) are observed early in the process and the entire range of resonances corresponding to all degrees of branching (Q¹–Q⁴) appear over time.^{19–20} For the case of base catalysis, hydrolysis is rate limiting and a high degree of branching is observed quickly. This is characterized in the ²⁹Si NMR spectra of evolving reactions by the presence of appreciable amounts of starting monomer late in the reaction and the immediate production of highly condensed species at Q³ and Q⁴. Notably, in base-catalyzed systems, modestly branched species at Q¹ and Q² are often not observed or appear in small amounts.^{22,23}

The temporal evolution of the ²⁹Si NMR spectrum of a 2.05 M solution of TMOS in the presence of a 5:1 water/silicon ratio, catalyzed by 2 mM Ni(acac)₂, is shown in Figure 2a. Soon after addition of water the broad resonance in the Q³–Q⁴ region at –110.3 ppm begins to increase in intensity. In addition, a small amount of monohydrolysis, Si(OCH₃)₃(OH), product at –75.7 ppm and monocondensed, Si–O–Si, species appear just upfield at –85.2 ppm (Q¹) are observed. As the reaction evolves, a steady increase in the intensity of the resonances in the region of the spectrum (Q⁴) corresponding to full condensation is observed. Notably, starting material remains in appreciable amount up through gelation. The reaction, run under identical conditions but catalyzed by an equivalent amount of OH⁻, is shown in Figure 2b. While the overall rate of the base-catalyzed

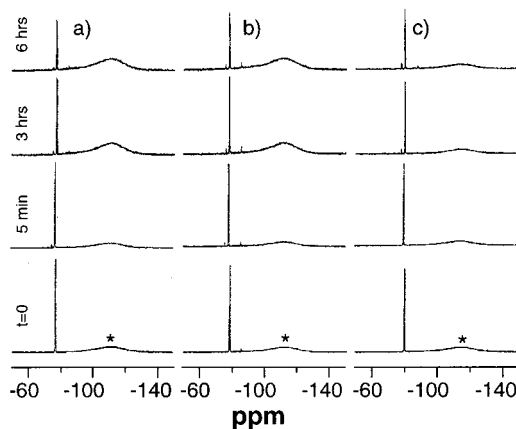


Figure 2. Temporal evolution of the ²⁹Si NMR spectrum of a 2.05 M solution of tetramethyl orthosilicate (5:1 water/silicon) catalyzed by 2 mM (a) Ni(II) bis(acetylacetonate), (b) sodium hydroxide, and (c) with no added catalyst (* indicates the background in the Q⁴ region contributed by the glass NMR tube).

reaction is slightly faster, the product distribution is exceedingly similar with the rapid formation of highly condensed material around Q³–Q⁴ and the presence of unreacted starting material late in the reaction with only very small amounts of weakly branched species (Q¹–Q²) observed. These data suggests that Ni(acac)₂ is acting primarily as a condensation catalyst. Similar product distributions were also observed for the Cu and Co bis(acetylacetonate) indicating that they act in the same manner. In comparison, when the reaction is run with no added catalyst (Figure 2c) it is extremely slow with no significant changes observed in the spectrum until 3 h into the process when small amounts of hydrolysis begin to be observed as evidenced by the characteristic peak at –75.7 ppm. After 6 h the amount of hydrolyzed monomer has increased while evidence of condensation becomes apparent in the Q¹ region. Notably, no changes in the Q²–Q⁴ region of the spectrum are observed suggesting that, unlike the OH⁻ and Ni(acac)₂-catalyzed solutions, condensation is the rate-determining step.

The pore structure of the final dried silica xerogels made with metal bis(acetylacetonate) catalysts is also consistent with condensation catalysis, which tends to yield significantly more mesoporous xerogels than are found when a hydrolysis catalyst is used. This mesoporosity arises from the large amount of highly branched silica that occurs with condensation catalysis.^{5–8} The nitrogen adsorption–desorption isotherms (Figure 3) for Ni(acac)₂ and OH⁻ are of type IV with a distinct type H2 hysteresis loop which is characteristic of capillary filling in mesoporous materials. In comparison, acid-catalyzed and uncatalyzed xerogels have isotherms that are unambiguously of type I with no hysteresis behavior.¹³ These differences are reflected in the values calculated from the isotherms (Table 3). Surface areas are larger and the total pore volumes smaller for the acid catalyzed and uncatalyzed control samples than for the Ni(acac)₂- and OH⁻-catalyzed materials. Estimates of the micropore volume of the materials, obtained from *t*-plot analysis, support the suggestion that the acid and uncatalyzed control samples are significantly more microporous. Interestingly, the Ni(acac)₂-catalyzed sample appears to produce a xerogel that has larger pores than a sample catalyzed with equivalent amounts of hydroxide.

Reaction Order and Thermochemical Parameters of M^{II}(acac)₂ Catalysts. A plot of the natural log of the reciprocal of the gelation times (ln(1/*t*_{gel})) versus the natural log of the concentration of the catalyst (ln[cat.]) is shown in Figure 4. This

(19) Kelts, L. W.; Armstrong, N. J. In *Better Ceramics Through Chemistry III*; Brinker, C. J., Clark, D. P., Beloeil, J. C., Lallemand, J. Y., Eds. *J. Non-Cryst. Solids* **1987**, *89*, 345.

(20) Pouxviel, J. C.; Boilot, J.; Beloeil, J. C.; Lallemand, J. Y. *J. Non-Cryst. Solids* **1987**, *89*, 345.

(21) Reference 3, p 160.

(22) Kelts, L. W.; Effinger, N. J.; Melpolder, S. M. *J. Non-Cryst. Solids* **1986**, *83*, 353.

(23) Reference 3, p 170.

Table 3. Effect of Catalysts on the Porosity of Silica Xerogels^a

catalyst ^b	surface area ^c (m ² /g)	pore volume ^d (cm ³ /g)	micropore volume ^e (cm ³ /g)	average pore size ^f (Å)
Ni(acac) ₂	373 (5)	0.64	0.02	69
OH ⁻	393 (8)	0.52	0.01	53
none	488 (3)	0.19	0.09	16
H ⁺	546 (2)	0.20	0.14	15

^a Samples made with 5:1 water and dried at 500 °C. ^b [Catalyst] = 0.002 M. ^c Calculated from the BET equation; this equation is not strictly applicable to microporous materials. ^d Calculated from density functional theory. ^e Derived from *t*-plot analysis. ^f Average pore size = 4V/A.

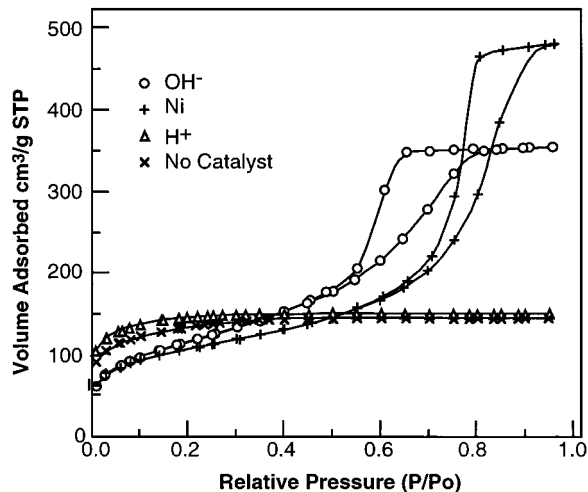


Figure 3. (a) Nitrogen adsorption–desorption isotherms for silica xerogels (5:1 water:silicon) made using no catalyst and catalyzed by Ni(II) bis(acetylacetonate), NaOH, and HCl at 2.0 mM.

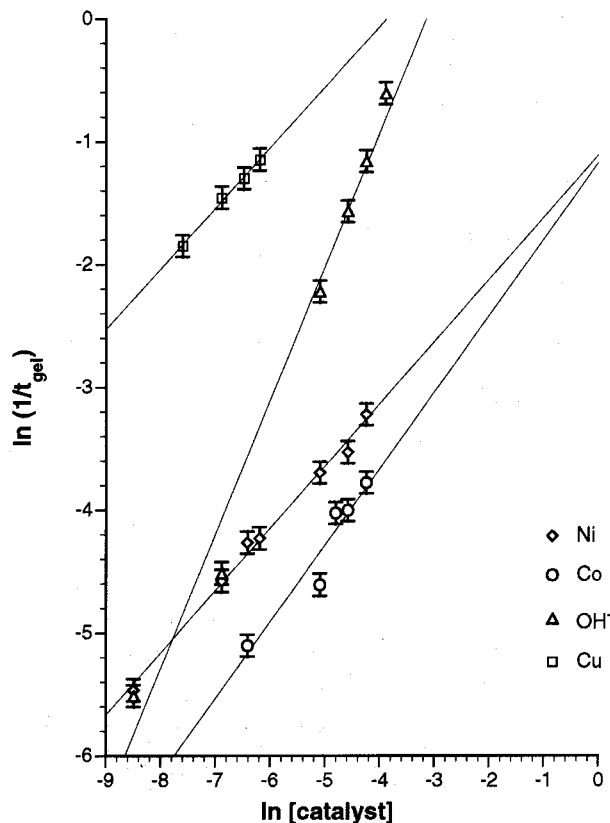


Figure 4. Plots of the natural log of the reciprocal of the gelation time vs the natural log of the catalyst concentration (note: OH⁻, Ni was run at 8:1 water/silicon while Co and Cu was run at 5:1).

plot is linear over the concentration range studied for all the catalysts (least-squares correlation coefficients ≥ 0.98). The slope of these plots, which corresponds to the order of the

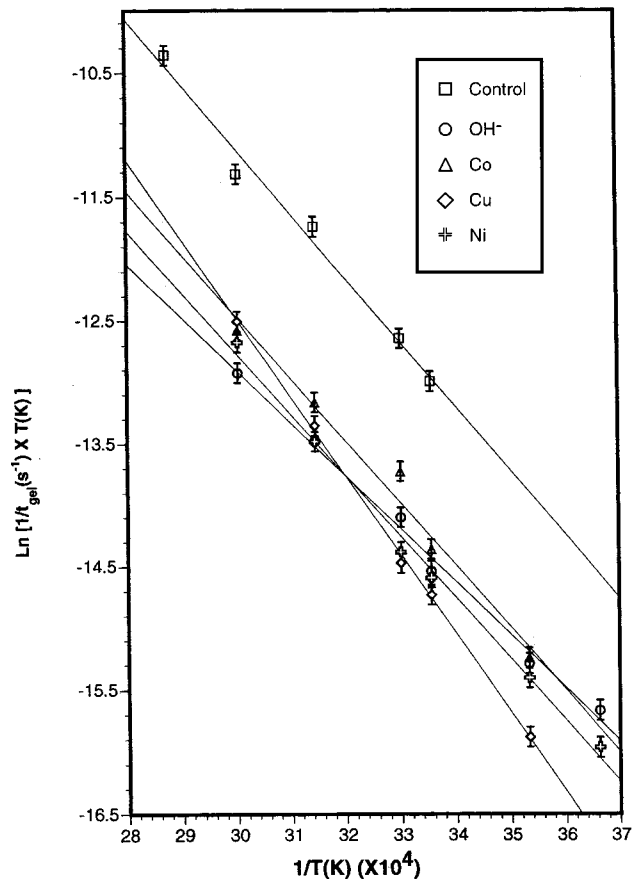


Figure 5. Eyring plots for tetramethyl orthosilicate (5:1 water/silicon) as catalyzed by NaOH, the bis(acetylacetonate complexes of Ni(II), Co(II), and Cu(II), and a control with no added catalyst.

reaction in added catalyst, is $1.09(\pm 0.02)$ for hydroxide while Ni, Co, and Cu bis(acetylacetonate) were determined to be $0.51(\pm 0.02)$, $0.55(\pm 0.02)$, and $0.49(\pm 0.02)$, respectively, suggesting a half-order dependence for the metal complex catalysts.

Figure 5 shows Eyring plots ($\ln[1/(t_{\text{gel}}T)]$) vs $1/T$ of identical sol–gel reactions as a function of temperature for Co, Ni, and Cu bis(acetylacetonate), hydroxide, and a control with no added catalyst. From the slope and intercept of the least-squares fit of the data the apparent activation enthalpy (ΔH^\ddagger) and entropy (ΔS^\ddagger), respectively, were determined, and from these values, the free energies of activation (ΔG^\ddagger) were calculated (Table 4).²⁴ Strictly speaking, the Eyring equation applies only to elementary reaction rate constants; hence, the thermochemical parameters obtained for the net rate of a complex reaction like the sol–gel process have no particular intrinsic significance except for use in comparisons within a homologous series such as this.

The Eyring plots show an isokinetic point for Cu(acac)₂, Ni(acac)₂, and OH⁻ catalysts at approximately 312 K while a

(24) Moore, J. W.; Pearson, R. G. *Kinetics and Mechanism*; Wiley: New York, 1981; p 177.

Table 4. Apparent Thermochemical Activation Parameters for Catalyzed Silica Sol–Gel Reaction^a

	catalyst				
	OH ⁻ ^b	Co(II) ^{b,c}	Ni(II) ^{b,c}	Cu(II) ^{b,c}	none
ΔH^\ddagger (kJ/mol)	36(1)	42(1)	41(1)	53(1)	43(1)
ΔS^\ddagger (J/mol K)	-198(1)	-175(1)	-180(1)	-142(1)	-194(1)
ΔG^\ddagger (kJ/mol) ^d	95(1)	94(1)	95(1)	95(1)	100(1)

^a Tetramethyl orthosilicate. ^b 2.0 mM. ^c Bis(acetylacetonate) complex, 2.0 mM. ^d Calculated from $\Delta G^\ddagger = \Delta H^\ddagger - T\Delta S^\ddagger$ for $T = 298$ K.

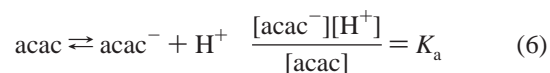
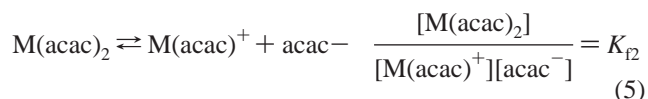
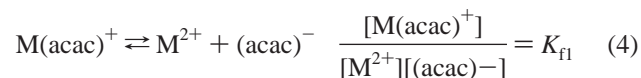
comparison of the thermochemical parameters (Table 4) appears to indicate a marked distinction between base and metal complex catalysis. In particular, hydroxide seems to have a markedly smaller activation enthalpy and a more negative activation entropy than the metal complexes. A more detailed analysis of the data, however, reveals that the isokinetic point and, more importantly, the apparent trends in activation enthalpy and entropy are artifactual and are a manifestation of the “compensation” effect. This arises in cases such as this one where differences in the free energy of activation (ΔG^\ddagger) are small for the whole series (Table 4). Under these conditions random errors in the determination of ΔH^\ddagger are automatically compensated for by concomitant changes in ΔS^\ddagger .^{25,26}

While the observed trends in the thermochemical parameters among the series of catalysts may not be reliable, the differences between individual catalysts and the uncatalyzed control are real.²⁷ The origin of the catalytic effect in the metal complexes does seem to arise from the entropic term, which is, on the whole, more positive than in the uncatalyzed sample while the activation enthalpies are approximately the same. When the same comparison is made between hydroxide and the control sample, the activation entropy is the same in both cases while the activation enthalpy is lower. It appears that the metal complexes afford a lower steric barrier to condensation than does hydroxide.²⁴ For both hydroxide catalysis and uncatalyzed sols, condensation would be expected to occur through the collision of two silicon alkoxide fragments in an S_N2 mechanism. In both systems a similar degree of steric congestion would likely exist in the transition state. The lower activation enthalpy observed in base catalysis can be attributed to the greater nucleophilicity of the siloxide species ($\equiv\text{SiO}^-$) which will be predominant under alkali conditions. The apparent dominance of the activation entropy in the catalytic activity of the metal bis(acetylacetonate) complexes suggests that the metal complexes in some fashion reduce that steric congestion during condensation.

Nature of the Active Catalyst. In the solid state, the Co(II) and Ni(II) bis(acetylacetonate) are respectively tetrameric and trimeric, while Cu(II) is monomeric.²⁸ In solution in noncoordinating solvents, the oligomeric structures are in equilibrium with monomeric species. In noncoordinating solvents, but in the presence of coordinating ligands, this equilibrium is pushed well to the right with the formation of 6-coordinate 2:1 adducts,

$\text{M}(\text{acac})_2\text{L}_2$.²⁹ Dissolution in donor solvents such as water or alcohol drives the equilibrium completely to the right, and in fact, recovering the oligomeric species from coordinating solutions requires rigorous dehydration.^{30,31} This suggests that, in the highly coordinating sol–gel solution, the active catalyst either is, or is derived from, an $\text{M}(\text{acac})_2\text{L}_2$ species where L is water, alcohol, or a silanol.

The pH of 2 mM aqueous solutions Co(II) and Ni(II) bis(acac) are basic yielding pH values of 9.33 and 9.24, respectively. This basicity arises from the ligand dissociation equilibria (eqs 4 and 5) of the complexes which generates the acetylacetonate anion whose equilibrium with water increases the pH (eq 6).



This raises the question of whether the observed catalytic activity is merely a trivial result of the metal-induced increase in pH. The magnitude of the catalytic effect seen with the metal complexes argues strongly against this. The fact that the catalysis rates for hydroxide and the Ni(II) and Co(II) complexes are comparable but that the pH of a 2 mM OH⁻ solution is significantly higher (pH = 11.3) seem to suggest that the pH resulting from metal complex dissociation is not sufficient to account for the catalysis. In fact a sol–gel solution made with OH⁻ concentrations of 0.02 mM which yields a pH value close to that induced by the Ni(II) and Co(II) complexes has a gelation time of 1620 min which is significantly longer than observed with the metal complexes.

As suggested, the active catalyst is likely to be either a 2:1 adduct of the bis(acac) complex, $\text{M}(\text{acac})_2\text{L}_2$, or a species arising from ligand dissociation. A comparison of the rate data and the formation constants for $\text{M}(\text{acac})_2$ complexes (Table 5) shows an inverse relationship (i.e. catalysis rate goes as Co > Ni > Cu and $K_{f1,2}$ values go Co < Ni < Cu). This indicates that the more highly dissociated the metal complex the greater its catalytic activity. Since our studies have shown that, at least for the case of Ni, the simple M^{2+} ions are ineffective catalysts when added independently, this implies that the monodissociated species, $\text{M}(\text{acac})^+$, is the active catalyst. This is a reasonable suggestion since ligand loss is frequently a first step in transition-metal-based homogeneous catalysis.³²

The key experimental parameter that distinguishes metal complex catalysis from base catalysis is the 1/2-order dependence of the rate on added metal complex. If the first dissociation product is the active catalyst, then this reaction order must be rationalized. Using reported values for the formation constants and the K_a of acetylacetonate, eqs 4–6 can be solved and the dependence of the metal species as a function of added $\text{M}(\text{acac})_2$ predicted.³³ Figure 6 shows a ln–ln plot of added solid Ni–

(25) Exner, O. In *Progress in Physical Organic Chemistry 10*; Streitwieser, A. S., Taft, R. W., Eds.; Wiley: New York, 1973; p 411.

(26) Evidence of the compensation in this case is obtained from plots of ΔH^\ddagger vs (ΔS^\ddagger) for the $\text{M}(\text{acac})_2$ and hydroxide-catalyzed solutions. These plots are very linear with a slope equal to the average temperature at which the data were acquired (306 vs 308 K, respectively). These observations, in conjunction with the constancy of the activation free energy, are strongly suggestive of the compensation effect (Halpern, J. *Bull. Chem. Soc. Jpn.* **1988**, *61*, 13).

(27) There is a large difference in ΔG^\ddagger between the catalyzed and uncatalyzed sols, and in plots of ΔH^\ddagger vs ΔS^\ddagger , the uncatalyzed sample deviates significantly from the trend line.

(28) Graddon, D. P. *Coord. Chem. Rev.* **1981**, *4*, 1.

(29) Ang, L. T.; Graddon, D. P. *Aust. J. Chem.* **1973**, *26*, 1901.

(30) Bullen, G. J.; Mason, R.; Pauling, P. *Inorg. Chem.* **1965**, *4*, 456.

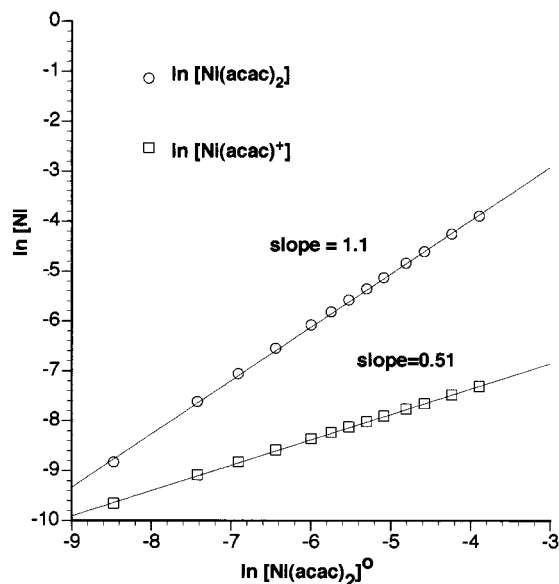
(31) Pfluger, C. E.; Burke, T. S.; Bednowitz, A. L. *Z. Cryst. Mol. Struct.* **1973**, *3*, 181.

(32) Cotton, F. A.; Wilkinson, G. *Advanced Inorganic Chemistry*, 4th ed.; Wiley: New York, **1980**; p 1265.

Table 5. Aqueous Formation Constants and Metal Speciation of $M(\text{acac})_2$ Calculated from Them

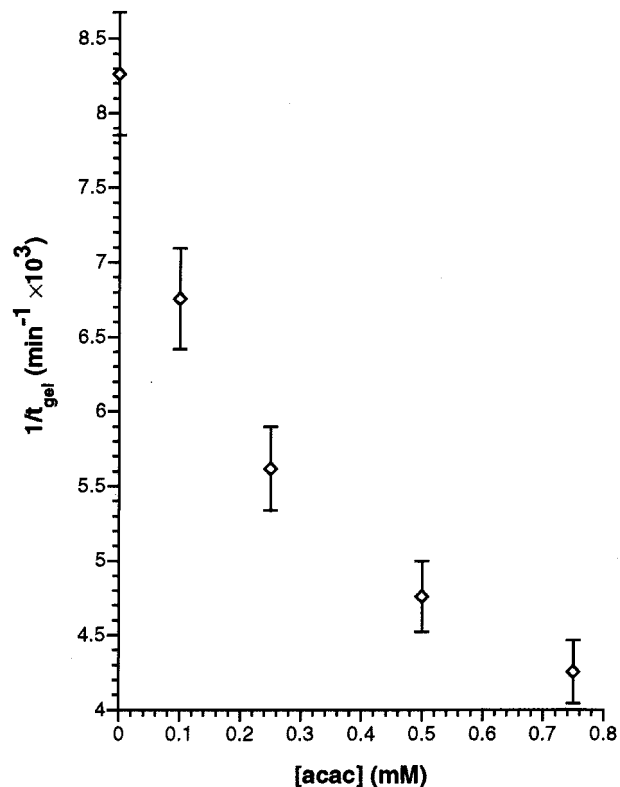
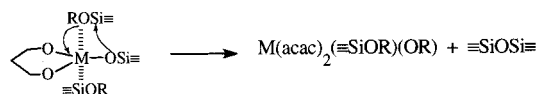
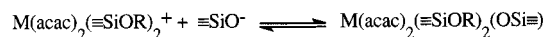
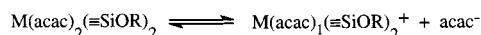
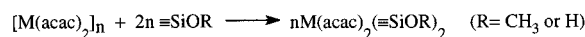
$[M(\text{acac})_2]^0$ 2.0 mM	$\log(K_{f1})^a$	$\log(K_{f2})^a$	pH calc ^b	$[M(\text{acac})_2]$ (mM)	$[M(\text{acac})^+]$ (mM)	rate ($1/t_{\text{gel}}$) ($\text{min}^{-1} \times 10^3$)	rate/ $[M(\text{acac})^+]$
Co	5.40	4.17	9.75	1.64	0.36	10.42	29
Ni	6.06	4.71	9.24	1.70	0.55	8.20	15
Cu	8.31	6.85	9.04	1.99	0.02	7.14	357

^a Values determined at 20 dC, ref 33. ^b Calculated for aqueous solutions using the $\text{p}K_a$ of acetylacetonate, 9.02 at 20 °C.³³

**Figure 6.** Plot of the natural log of the calculated $\text{Ni}(\text{acac})_2$ and $\text{Ni}(\text{acac})^+$ concentrations predicted in aqueous solution as a function of the natural log of added solid $\text{Ni}(\text{II})$ bis(acetylacetonate).

$(\text{acac})_2$ vs the concentration of $\text{Ni}(\text{acac})_2$ and $\text{Ni}(\text{acac})^+$ in equilibrium as calculated from the equations. The concentration range selected (0.2–20 mM) corresponds to that used in the gelation experiments. As shown in the graph, the first dissociation product, $\text{Ni}(\text{acac})^+$, is produced with an apparent $1/2$ order dependence on added $\text{Ni}(\text{acac})_2$ over this range. The other complexes, Co and Cu, showed a similar dependence, and in all cases, changes in $M(\text{acac})_2$ and in pH were not of $1/2$ order. It is important to emphasize, however, that the calculations are based on formation constants determined in aqueous media. These constants may differ in the sol–gel solution; however, calculations using formation constants that varied over several orders of magnitude indicate that the functional dependence of the $M(\text{acac})^+$ species on added metal complex varies slowly and remains $1/2$ order within the error of the gelation measurements.³⁴

If the $M(\text{acac})^+$ species is, in fact, the active catalyst, then we would predict that the addition of excess acetylacetonate should force the equilibria to the left thereby reducing the amount of $M(\text{acac})^+$ and inhibiting the reaction. Inhibition is observed (Figure 7) in the case of the $\text{Ni}(\text{acac})_2$ system where the gelation times become significantly longer upon the addition of very small amounts of acetylacetonate. While this result supports the suggestion that $\text{Ni}(\text{acac})^+$ is the active catalyst, it must be taken with some caution since the addition of

**Figure 7.** Plot of the reciprocal of the gelation time of a 2.0 mM $\text{Ni}(\text{acac})_2$ -catalyzed solution (5:1 water/silicon) as a function of added acetylacetonate (acac).**Scheme 1**

acetylacetonate will also lower the pH which will also act to inhibit gelation. However, the predicted pH changes are small and would not be expected to have such a dramatic effect on the gelation time.

Since the gelation rate increases with the quantity of $M(\text{acac})^+$ in solution (Table 5), it is interesting to determine whether the catalytic activity is also dependent on the nature of the metal. The ratio of the gelation rate to the calculated amount of $M(\text{acac})^+$ (Table 5) indicates that the rate per mole of catalyst is actually highest for Cu.

Mechanism of the Reaction. Due to the inherent complexity of the sol–gel process, detailed mechanistic studies are difficult. However, a rather straightforward mechanism (Scheme 1) can be suggested on the basis of the dissociation processes described

(33) Izatt, R. M.; Fernelius, W. C.; Block, B. P. *J. Phys. Chem.* **1955**, *59*, 80.

(34) The formation constants for $\text{Ni}(\text{acac})_2$ in mixed alcohol/water solvent systems, which more closely resemble the sol–gel solution, have been determined (Gentile, P. S.; Dadgar, A. *J. Chem. Eng. Data* **1968**, *13*, 367) and tend to be larger than those reported in water. Calculations utilizing these higher constants produced the same apparent $1/2$ -order functional dependence.

above and the known coordination chemistry of square-planar metal diketonates. The dissolved $M(\text{acac})_2$ complex is initially present as the 6-coordinate 2:1 adduct, $M(\text{acac})_2L_2$, where L can be a silanol as indicated in the scheme. This complex dissociates a ligand and coordinates a siloxide in the vacant coordination site. This is followed by an insertion that displaces the hydroxy/alkoxy group to the metal. The essential feature of this mechanism is that the metal acts as a template which brings the silicon groups together and, because of its intermediacy, reduces the steric strain. Clearly, other mechanisms can be offered though the basic aspects of this one are consistent with the data.

Conclusion

In conclusion, this study shows that transition-metal complexes, in particular the metal bis(acetylacetonate), can act as efficient catalysts for the sol–gel process. These complexes appear to act primarily as condensation catalysts and are,

therefore, comparable to hydroxide in their activity. The use of these metal complexes as sol–gel catalysts may find practical application in doped sol–gel materials where conventional acids and bases are unsuitable. Finally, since metal acetylacetonate complexes are often used to introduce late transition metals into the silica matrix, the fact that they are not benign dopants but, in fact, significantly alter the properties of the xerogel is of importance in the fabrication of metal–silica glasses.

Acknowledgment. We thank Dr. Tom Gedris for assistance in acquiring NMR spectra. We are appreciative to Dr. Rick Finke for his many insightful comments which contributed greatly to this paper. Support for E.I.M. was provided by a University Fellowship of The Florida State University. Support of D.D.P. was provided by the National Science Foundation. Funding for this research was provided by the National Science Foundation under Grant DMR-9623570.

IC990577L